

Article

# A Study of Minimum Quantity Lubrication (MQL) by Nanofluids in Orbital Drilling and Tribological Testing

Mohsen Mosleh <sup>1</sup>, Khosro A. Shirvani <sup>2,\*</sup>, Sonya T. Smith <sup>1</sup>, John H. Belk <sup>3</sup> and Gary Lipczynski <sup>4</sup>

<sup>1</sup> Mechanical Engineering Department, Howard University, Washington, DC 20059, USA; mmosleh@howard.edu (M.M.); ssmith@howard.edu (S.T.S.)

<sup>2</sup> Mechanical Engineering Department, Rowan University, Glassboro, NJ 08028, USA

<sup>3</sup> Zero Technology LLC, Blue Ridge, GA 30513, USA; jhbelk@gmail.com

<sup>4</sup> The Boeing Company, Hazelwood, MO 63042, USA; gary.lipczynski@boeing.com

\* Correspondence: Khosro.A.Shirvani@gmail.com; Tel.: +1-202-746-9766

Received: 4 December 2018; Accepted: 5 January 2019; Published: 11 January 2019



**Abstract:** In minimum quantity lubrication (MQL), an aerosol containing a minimum amount of the cutting fluid is delivered to the tool/workpiece interface during the metal cutting operation. The fluid lubrication by the fluid and the cooling by the compressed air in the aerosol improves the cutting process, while the low consumption rate in MQL provides less cleanup and reduces the associated cost. In this paper, molybdenum disulfide (MoS<sub>2</sub>) and hexagonal boron nitride (hBN) nanoparticles were added to the aerosol for providing a third functionality to the MQL, which is solid lubrication at the interface. Both orbital drilling and tribological testing using a four-ball tester were studied to examine the effectiveness of solid lubrication in MQL. In orbital drilling of titanium with tungsten carbide tools, MQL with nanofluids containing MoS<sub>2</sub> nanoparticles resulted in less transfer film buildup on the tool. In four-ball testing, MQL with nanofluids with MoS<sub>2</sub> and hBN nanoparticles yielded lower surface temperatures and less variation of frictional torques in titanium.

**Keywords:** nanofluid; MQL; orbital drilling; four-ball testing

## 1. Background

In the context of cooling and lubrication by cutting fluids, the notion of “the more, the better” is giving way to stricter environmental regulations and research findings in recent years in the effectiveness of minimum quantity lubrication (MQL) in lieu of flood lubrication. In MQL, a minute amount of the cutting fluid with an approximate flow rate range of 5–50 mL/h is mixed with compressed air and delivered as aerosol to the tool/workpiece interface [1]. The lubricating function is achieved by the cutting fluid, while the cooling function is mainly ensured by the high flow-rate of the compressed air [2]. Due to evaporation of the small amount of the cutting fluid in MQL upon contact with the hot tool–interface spot, the residues of the cutting fluid on the workpiece and chip surfaces is minimal. The low consumption of the cutting fluid in MQL can yield reduced waste disposal and chip treatment [3], improved occupational safety [4,5], and enhanced environmental compatibility [6]. Considering that the cutting fluid cost is reported to be higher in the automotive industry than that of the cutting tool cost, the low consumption rate in MQL presents an enormous cost-saving potential [7–9]. In addition to economic efficiency and environmental compatibility, the MQL has been reported to meet or exceed flood lubrication performance in terms of tool life and surface quality of the workpiece [10]. Specifically, in drilling of AISI 4340 with oxide-coated HSS drill bits using a vegetable oil in flood lubrication and MQL, no significant tool life difference, measured by the number of holes before reaching the end of life criterion, was observed. Additionally, the average thrust force was lower

in drilling with the MQL [10]. In milling of high strength steel with cemented carbide tools and end milling of stainless steel using TiAlN coated nitride tools, MQL reduced the tool wear and surface roughness compared with dry and flood-lubricated cutting [11,12].

Nanofluids as colloidal dispersions of various nanoparticles in a base cutting fluid have been examined for machining operations such as milling, drilling, grinding, and turning [13,14]. Since nanofluids containing various oxides, carbides, and carbonic and metallic nanoparticles have exhibited marked enhanced thermal conductivity compared to the base fluid, the cooling functionality of cutting nanofluids in flood lubrication is improved and, therefore, the cutting temperature is reduced [15–17]. Nanofluids containing molybdenum disulfide ( $\text{MoS}_2$ ), graphite, tungsten disulfide ( $\text{WS}_2$ ), and other nanoparticles with a lamellar structure have also exhibited lower friction compared to the base fluid. The lower friction is attributed to solid lubrication by lamellar-structured nanoparticles, which provide an easy shearing surface between contacting surfaces [13,18–20]. Additionally,  $\text{MoS}_2$  nanoparticles in nanofluids have been shown to form a tribofilm, resulting in lowering friction, and to deagglomerate wear particles for reduced transfer films [21,22]. Recently, the use of nanofluids containing graphite, carbon nanotubes (CNT),  $\text{MoS}_2$ , and hexagonal boron nitride (hBN) in MQL has been reported for various machining operations, including turning and grinding with improved tool life, surface quality, and heat dissipation [23–26].

The application of MQL in emerging machining processes, such as high-speed drilling and orbital drilling, has shown promising results for hard-to-machine materials, such as hardened steel, aerospace alloys, carbon-fiber reinforced plastic (CFRP), and titanium/CFRP laminates, in terms of workpiece surface quality and reduced surface [8,27,28]. Orbital drilling represents a promising alternative drilling process with advantages over conventional drilling, such as reduced tool inventory, reduced axial force and risk for delamination in composite laminates, better cooling of the tool and hole edges, and the ability to repair misaligned and damaged holes. The incorporation of MQL in orbital drilling also reduces operational costs through the minimal use of the fluid and lack of residues [29–31].

This paper presents the results of an investigation on the three functionalities of MQL by nanofluids, i.e., fluid lubrication, cooling, and solid lubrication, in orbital drilling and tribological testing at a flow rate of 2 mL/h, which is less than the flow rate in MQL with conventional fluids. The solid lubrication by nanoparticles and its tribological effect were examined with the reduced flow rate in MQL by nanofluids. The evidence of effectiveness of these functionalities are presented and discussed with suggestions for further improvements. The investigation of MQL by nanofluids for orbital drilling, which is an emerging machining process in aerospace applications, has not been previously addressed in the literature and presents a new opportunity for future studies.

## 2. Experimental Method

### 2.1. Nanolubricant Preparation

The base fluid in this investigation was Boelube 70104, manufactured by Orelube Inc (New York, NY, USA) Boelube is a commonly used proprietary long chain alcohol-based liquid machining lubricant, which does not contain any ingredients that the Occupational Safety and Health Administration (OSHA), Workplace Hazardous Materials Information System (WHMIS), International Agency for Research on Cancer (IARC), National Toxicology Program (NTP), or U.S. State Regulatory Lists consider hazardous [32]. The primary use of Boelube is in minimum quality lubrication. Boelube-based dispersions were prepared by the addition of nanoparticles to the base fluid and sonication by a sonicator probe for approximately 15 min at 20 W output. In order to prevent significant heating of the nanofluid sample during sonication, the container of the fluid sample was placed in a bath of iced water. A 1-mL sample of the nanofluid was examined by light scattering to determine the dynamic equilibrium particle size. Table 1 shows the physical characteristics of hBN and  $\text{MoS}_2$  nanoparticles and their average dynamic equilibrium size in the nanofluid before and after sonication. As Table 1 shows, the sonication reduced the average dynamic equilibrium size of the particles in the nanofluid

compared with mechanical shaking, but it did not fully deagglomerate the particles in the nanofluid to the individual particles in the powder.

**Table 1.** Nanoparticles and their dispersion characteristics.

Materials	Average Size (nm) as Powder	Average Size (nm) in Boelube after Shaking	Average Size (nm) in Boelube after Sonication
MoS <sub>2</sub> nanoparticles	70–100	800	550
hBN nanoparticles	70	750–850	550

### 2.2. Mist Pump

A positive displacement pump with individually adjustable air and fluid volumes made by UNIST, Inc. (Grand Rapids, MI, USA) was used for producing a continuous mist output. The fluid and air were combined at the nozzle tip for consistent atomization. The nanofluids were prepared in advance and were continuously mixed using a mechanical mixer while in the reservoir of the mist pump to prevent particle settlement. The fluid flow rate for a given dial setting was measured by collecting the output fluid in the mist for a given period. The fluid flow rate in milliliter per hour was then calculated. Additionally, the air flow rate was measured by collecting the mist output in a balloon and measuring its volume for a given period, as shown in Figure 1. MoS<sub>2</sub> and hBN were used as effective solid lubricants for improved tribological properties. To vent out any remnant mist of nanolubricants containing MoS<sub>2</sub> and hBN nanoparticles, a fume hood with an exhaust flow rate of 0.2 cm<sup>3</sup>/s was used in laboratory tests.

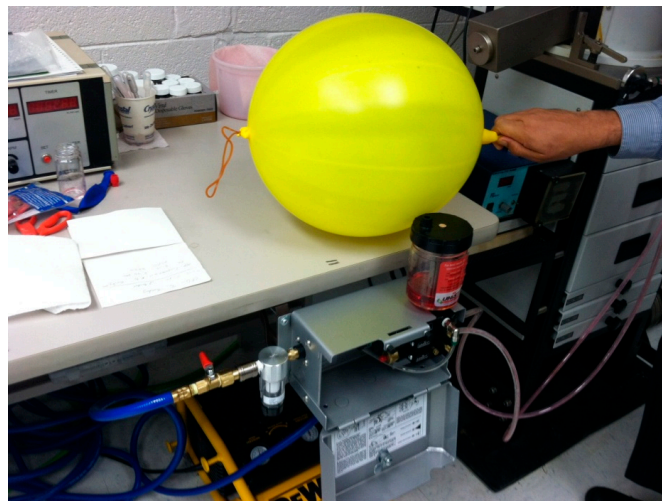


**Figure 1.** Balloon method for measuring the air flow rate from the mist pump.

### 2.3. Orbital Drilling

In the orbital drilling setup, the cutting tool rotates about its own axis and eccentrically about a principal axis, while the tool feeds through the material for machining a hole. The setup was equipped with a vacuum-based chip evacuation system and used MQL and pressurized air through the spindle [29]. The process parameters included a cutting speed of 1.0 m/s, a lubricant flow of 2 cm<sup>3</sup>/h, and a pressurized air flow of 944 cm<sup>3</sup>/s. The tool was made of tungsten carbide and the workpiece was a titanium 6Al4V (Ti) plate of 12.7-mm thickness. A schematic of the setup is shown in Figure 2.

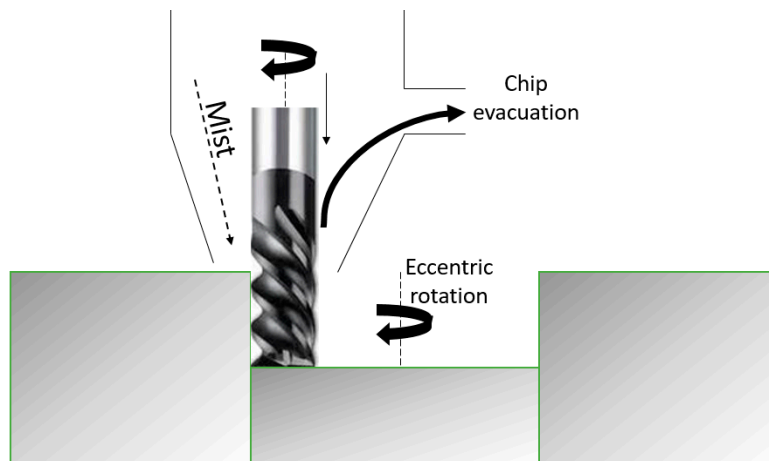


Figure 2. Schematic of the orbital drilling setup.

### 2.4. Four-Ball Testing

A modified brand model four-ball tester with a maximum rotational speed and normal load of 10,000 rpm and 10,000 N, respectively, was used. Through the system’s computer interface, the test conditions, such as speed, load, and oil temperature, were controlled and recorded during the tests. The ball configuration and geometry are shown in Figure 3. The lower balls are fixed, and the upper ball rotates with a rotational speed so that the relative linear speed at the contact points was 1.0 m/s. The upper ball, which represents the tool in orbital drilling, was made of tungsten carbide (WC). The lower balls, which represent the workpiece, were titanium. The ball specifications are shown in Table 2. The temperature of the top ball was measured by a FLIR i3 infrared camera (IR) with a  $60 \times 60$  IR resolution, manufactured by FLIR Systems Inc. (Wilsonville, OR, USA), approximately 3 s after the test was completed. The applied load was chosen so that the Hertzian contact stress was 3.5 GPa. The MQL conditions comprised of  $2 \text{ cm}^3/\text{s}$  lubricant flow within an air flow of  $236 \text{ cm}^3/\text{s}$ .

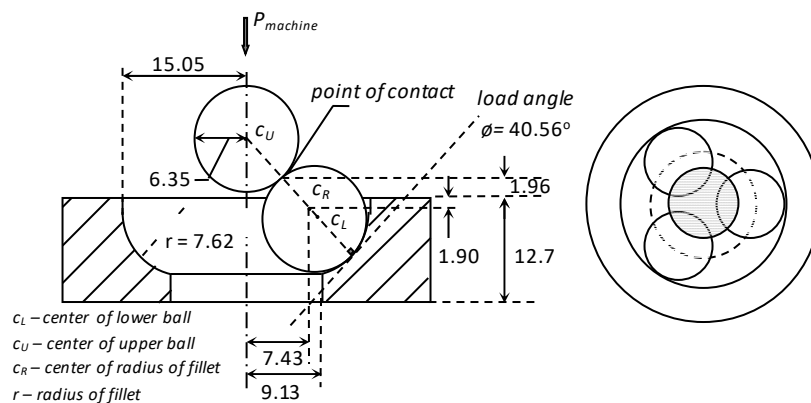


Figure 3. Four-ball test setup and the ball configuration and geometry. All dimensions are given in mm.

Table 2. Ball specifications.

Ball	Diameter (mm)	Grade	Arithmetical Mean Roughness $R_a$ (nm) (ISO 4287:1997)
Tungsten Carbide (WC)	12.7	25	50
Titanium 6Al4V (Ti)	12.7	200	200

### 3. Experimental Results and Discussion

#### 3.1. Results from Orbital Drilling

The cutting edges of four different WC tools, out of a total of 6 tools, machining Ti samples, which were taken in a JEOL JSM-7600F field emission scanning electron microscope (SEM) with integrated energy dispersive spectroscopy (EDS), are shown in Figure 4. The maximum height of the worn area of the WC tool is 182  $\mu\text{m}$  for Boelube and 149  $\mu\text{m}$  for the nanofluid containing 2% of  $\text{MoS}_2$  by weight. The images on the left side were with pure Boelube and the ones on the right side were with the nanofluid. It appears that when pure Boelube was used, the transfer film on the edges of the tools was formed. On the other hand, the transfer film was less on the edges of the cutting tool with the nanofluid. Energy dispersive spectroscopy (EDS) of cutting edges of the WC tools used for machining Ti samples was performed. Figure 5 shows one of the ten spectrums of cutting edge of a WC tool, which machined Ti with pure Boelube. The elemental analysis of surface of the edge in nine spectrums is shown in Table 3. The analysis points to the fact that in an average of nine different examination spots, over 63% of the elements on the surface are titanium, aluminum, and vanadium, which are from a 6Al–4V titanium workpiece. Tungsten (W) accounts for approximately 27% of the elements on the tool surface. In comparison, Figure 6 shows one of the nine spectrums of cutting edge of a WC tool, which machined Ti with the nanofluid. The elemental analysis of surface of the edge in ten spectrums is shown in Table 4. In this case, approximately 36% of the elements on the surface are titanium, aluminum, and vanadium, which are from a 6Al–4V titanium workpiece, while tungsten accounts for 32% of the elements.

Based on the elemental analysis of tool surfaces by EDS, the use of nanofluids containing  $\text{MoS}_2$  nanoparticles resulted in less material transfer and edge buildup from the workpiece containing titanium, aluminum, and vanadium on the tungsten carbide tool. Additionally, the elemental percentage of tungsten was increased in the EDS spectra as the tungsten carbide tool surface contained less transfer film from the workpiece.

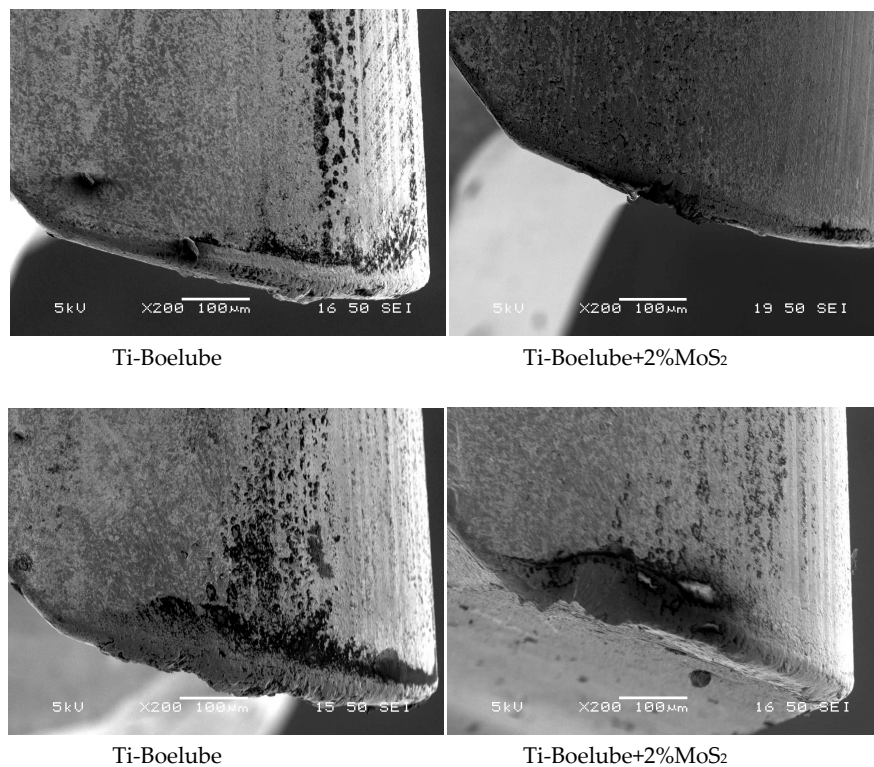


**Figure 4.** SEM micrographs of cutting edges of two sets of tungsten carbide (WC) tools when cutting Ti with Boelube and Boelube+2% $\text{MoS}_2$ .

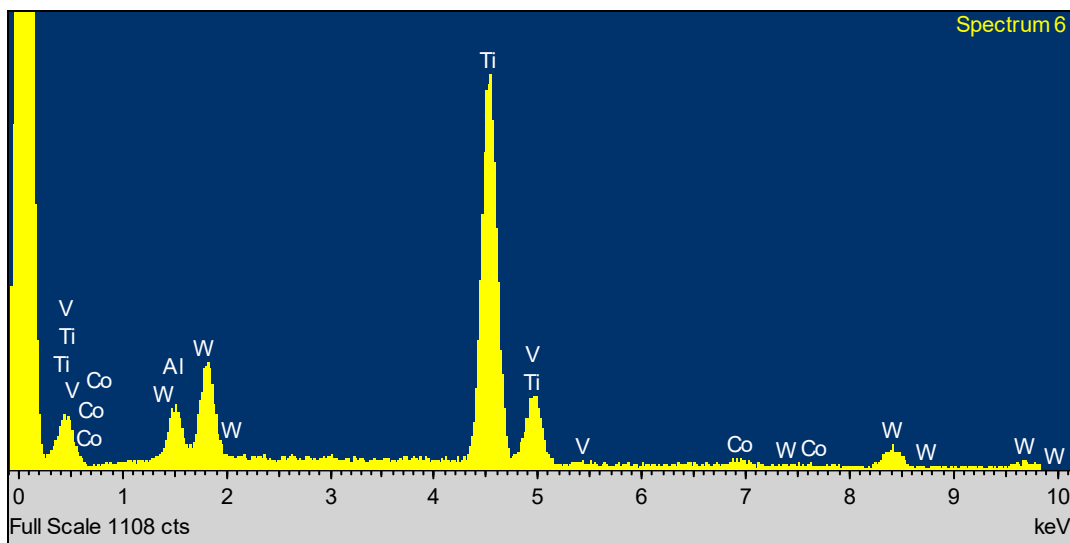


Figure 5. Energy dispersive spectrometry (EDS) spectrum of edges of a WC tool cutting Ti with pure Boelube.

Table 3. Elemental analysis of surface of the edge of a WC tool cutting Ti with pure Boelube.

WC Tool (with Pure Boelube) (all Results in Weight%)								
Spectrum	In stats.	Al	Ca	Ti	V	Co	W	Total
Spectrum 2	Yes	-	-	1.12	-	-	-	1.12
Spectrum 3	Yes	4.59	-	71.66	3.65	1.19	7.04	88.13
Spectrum 4	Yes	2.41	-	34.89	-	5.13	36.65	79.08
Spectrum 5	Yes	5.04	-	61.73	2.54	-	6.05	75.35
Spectrum 6	Yes	4.08	-	53.33	2.83	1.76	19.1	81.1
Spectrum 7	Yes	9.11	-	90.44	2.6	-	-	102.16
Spectrum 8	Yes	3.36	0.79	38.58	1.44	5.62	59.02	108.8
Spectrum 9	Yes	6.11	-	72.4	3.68	3.7	32	117.88
Spectrum 10	Yes	5.58	-	68.49	3.61	2.21	32.28	112.17
Max.	-	9.11	0.79	90.44	3.68	5.62	59.02	-
Min.	-	2.41	0.79	1.12	1.44	1.19	6.05	-
-	Average	5.0	-	54.7	2.9	-	27.4	-

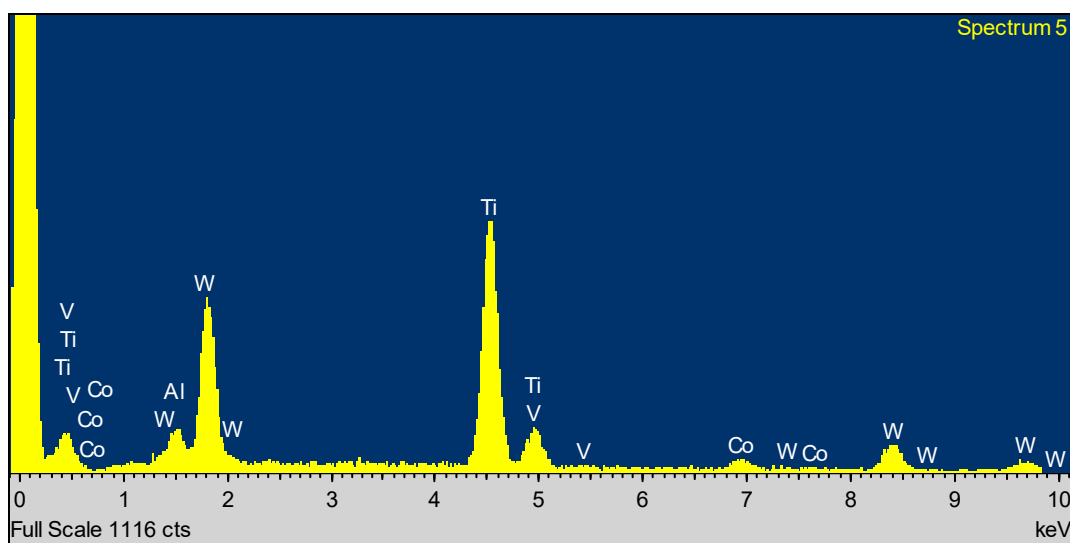
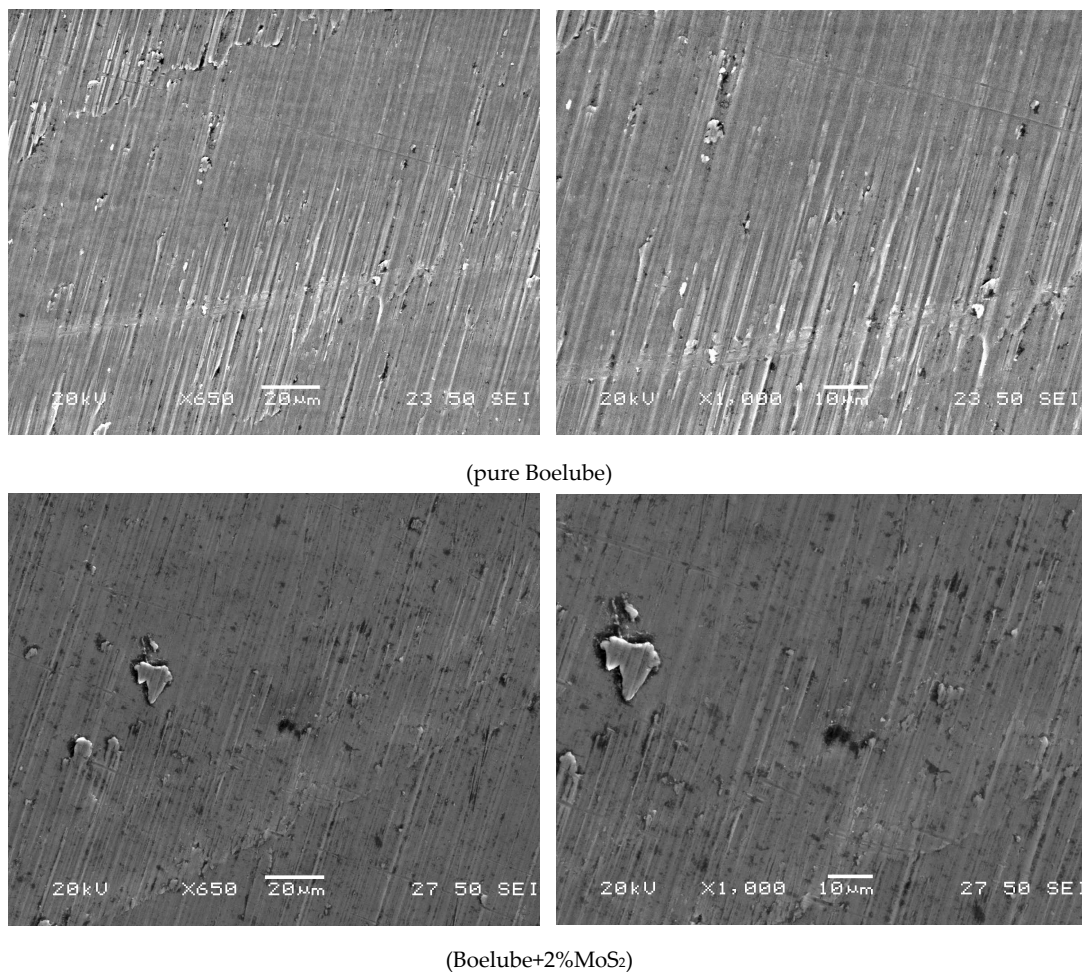


Figure 6. EDS spectrum of edges of a WC tool cutting Ti with Boelube+2%MoS<sub>2</sub>.

**Table 4.** Elemental analysis of surface of the edge of a WC tool cutting Ti with Boelube+2%MoS<sub>2</sub>.

WC Tool (with Boelube+2%MoS <sub>2</sub> ) (all Results in Weight %)								
Spectrum	In stats.	O	Al	Ti	V	Co	W	Total
Spectrum 1	Yes	-	0.57	5	-	6.99	59.89	72.44
Spectrum 2	Yes	-	0.79	6.99	-	6.25	59.77	73.81
Spectrum 3	Yes	-	0.84	19.56	0.9	2.11	15.72	87.91
Spectrum 4	Yes	-	-	11.19	-	1.06	2.27	14.51
Spectrum 5	Yes	-	2.19	33.72	1.09	2.53	30.02	69.55
Spectrum 6	Yes	-	2.3	53.42	2.64	0.84	4.96	64.15
Spectrum 7	Yes	6.07	1.06	8.6	0.87	3.48	71.5	91.57
Spectrum 8	Yes	-	5.86	73.98	2.83	-	6.68	89.34
Spectrum 9	Yes	-	4.78	59.41	2.56	2.72	24.69	94.15
Spectrum 10	Yes	-	3.69	44.08	2.7	3.89	45.94	100.3
Max.	-	6.07	5.86	73.98	2.83	6.99	71.5	-
Min.	-	6.07	0.57	5	0.87	0.84	2.27	-
-	Average		2.5	31.6	1.9	-	32.1	-

Machined titanium surfaces examined by a scanning electron microscope (SEM) are shown in Figure 7. The SEM images were taken at 650× and 1000× magnifications. The titanium surfaces machined using the nanofluid appear to have adhered wear debris. This wear debris was shown by the SEM and EDS analysis of Figures 5 and 6 and Tables 3 and 4 to adhere to the WC tools in the absence of using nanofluids.



**Figure 7.** SEM micrographs of Ti workpiece surfaces machined using Boelube and Boelube+2%MoS<sub>2</sub>.

### 3.2. Results from Four-Ball Testing

The frictional torque and the IR temperature profile of the top ball assembly at the end of the test with WC/Ti pairs for Boelube and the nanofluid with MoS<sub>2</sub> nanoparticles is shown in Figure 8. The frictional torque for pure Boelube has significant fluctuations and higher peaks, especially in the second half of the test. The surface temperature of the tungsten carbide ball at the center of the crosshair, measured 3 s after the test ended, was 233 °C and 180 °C when using Boelube and nanofluid containing MoS<sub>2</sub>, respectively. The reduction of surface temperature in three tests with nanofluid containing MoS<sub>2</sub> was consistently around 20%. Figure 9 exhibits a similar pattern of smoother torque with lower peaks, but without a marked lower surface temperature when the nanofluid with the hBN nanoparticles were used, compared to the corresponding values for Boelube as the lubricant. The surface temperature of the upper balls was found experimentally to reach to a steady state after approximately 9 min (560 s). Therefore, the surface temperature at the crosshair shown in Figures 8 and 9 represents the steady state temperature of the top ball in each test.

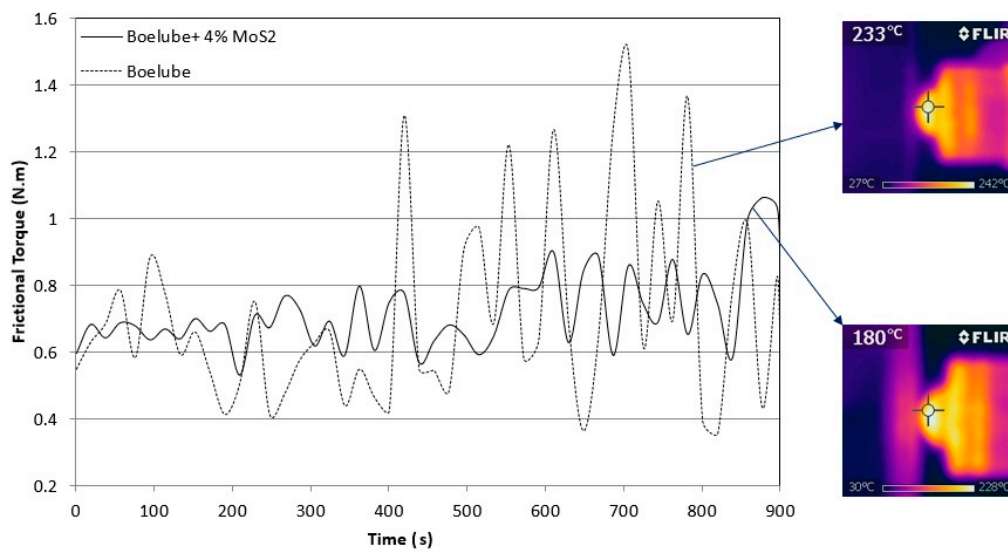


**Figure 8.** Frictional torque and surface temperature of the top WC ball against Ti lower balls at 3.5 GPa contact stress for Boelube and Boelube with MoS<sub>2</sub> nanoparticles.

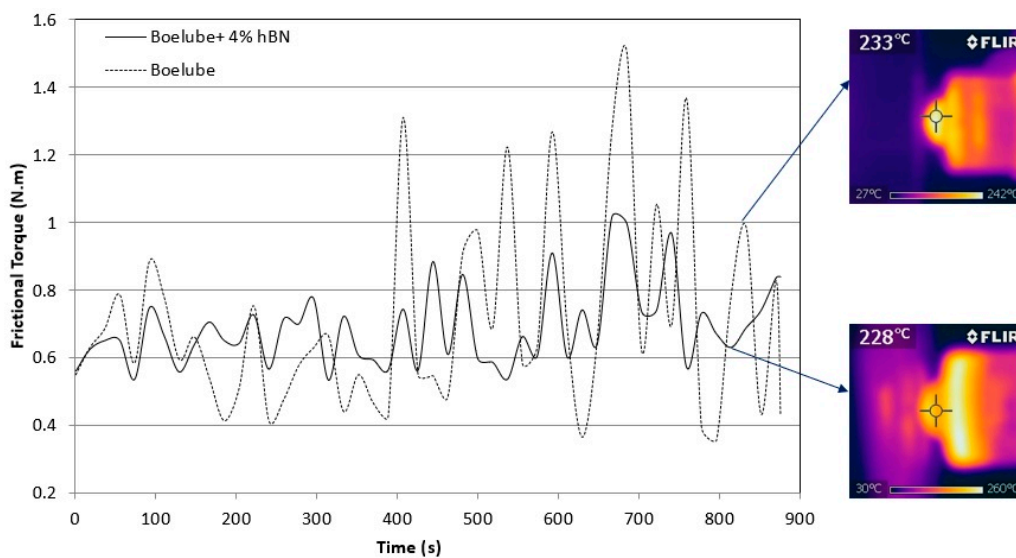


**Figure 9.** Frictional torque and surface temperature of the top WC ball against Ti lower balls at 3.5 GPa contact stress for Boelube and Boelube with hBN nanoparticles.



With respect to wear, the tungsten carbide upper balls did not experience a measurable wear during the 15-min four-ball tests for both Boelube and nanofluids. The average of wear mass of titanium lower balls in three tests with each of the nanofluids and in five tests with Boelube and the corresponding standard deviation of the wear mass data as the error bar are shown in Figure 10. The existence of MoS<sub>2</sub> and hBN nanoparticles in the MQL mist has reduced the sliding wear in the softer material, i.e., titanium. Several mechanisms through which dispersed nanoparticles with a lamellar structure, such as MoS<sub>2</sub> and hBN in nanolubricants and nanofluids, result in lower friction and wear are contemplated in the literature. These mechanisms include the formation of a transferred solid lubricant film [33], easy shearing of trapped nanoparticles at the interface [34], rolling of spherical nanoparticles in the contact zone and reducing asperity contact by filling the valleys of contacting surfaces [35], and deagglomeration of wear particles and reducing plowing by wear particles [13,36]. The lower wear results obtained here are also consistent with extreme pressure testing of nanofluids containing MoS<sub>2</sub> and hBN [37–39].

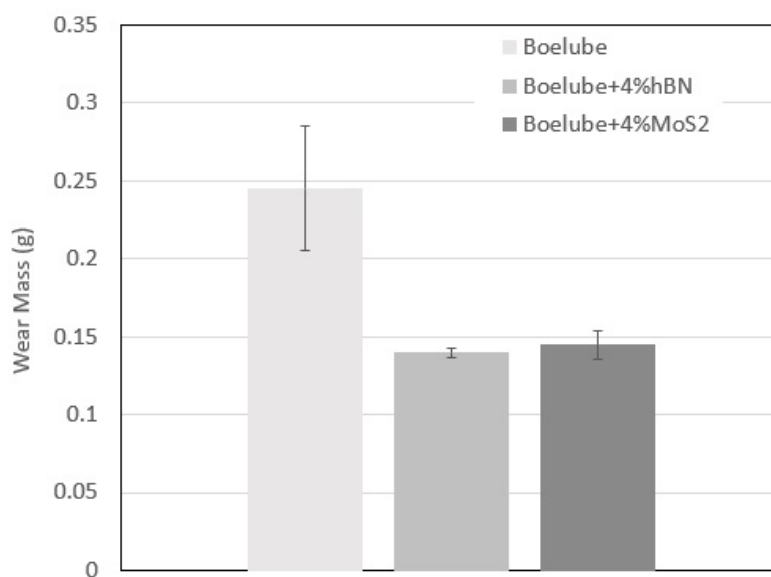


**Figure 10.** Wear of titanium lower balls.

In this study, the orbital drilling tests were conducted prior to 4-ball testing. To avoid clogging the mist pump during orbital drilling tests, a nanoparticle concentration of 2% was chosen. As the mist pump operated with nanofluids without clogging, the nanoparticle percentage was increased to 4% in 4-ball testing. Nevertheless, in both the orbital drilling and 4-ball testing, a comparative analysis shows improvement in characteristics, such as less transfer film on the WC tool, a smoother frictional torque, and lower surface temperature from Boelube to nanofluids containing MoS<sub>2</sub> nanoparticles. One limitation of this investigation was the surface temperature measurement technique using the IR camera. The measurement was extremely sensitive to the time after the test stoppage. Numerous attempts were made to perfect the temperature measurement procedure for consistency. A more robust method of temperature measurement, such as embedded thermocouples in fixed lower ball samples, can provide a continuous, more reliable surface temperature reading. The less transfer film on the WC tools in orbital drilling and smoother frictional torque with a lower surface temperature in four-ball testing using nanolubricant containing MoS<sub>2</sub> and hBN with lamellar structure support the model of wear debris deagglomeration, which results in lower plowing wear, less friction, and lower fluctuations in the frictional force and torque [22].

#### 4. Conclusions

Molybdenum disulfide (MoS<sub>2</sub>) nanoparticles dispersed in Boelube exhibited the ability to reduce the buildup of the Ti transfer film on WC tools in orbital drilling. In laboratory four-ball tests, nanofluids with dispersed MoS<sub>2</sub> and hBN nanoparticles resulted in less frictional torque variation with lower peaks. The antiwear properties of these nanoparticles that were previously reported in the literature for flood lubrication in extreme pressure testing were also observed in MQL in this study. The use of nanofluids resulted in less wear on lower titanium balls in four-ball testing under MQL conditions. Overall, MQL with nanofluids provided fluid lubrication, cooling, and solid lubrication for process improvement with less cleanup. Due to the low fluid flow rate in MQL, a very small amount of nanoparticle additives is delivered to the contact zone. Therefore, the effectiveness of nanofluids can be increased by reducing the nanoparticle size. The reduction in the nanoparticle size increases the available nanoparticles in a given volume and provides a higher surface area for interaction at the interface.

**Author Contributions:** Supervision, Methodology, Writing—original draft preparation, M.M.; Investigation, writing—review and editing K.A.S. and S.T.S.; Project administration, conceptualization, funding acquisition, J.H.B. and G.L.

**Funding:** This work was supported by The Boeing Corporation under contract TBC-HU-GTA-1 (RA-8).

**Acknowledgments:** The authors acknowledge James Griffin of Howard Nanoscience Facility (HNF) and Keron Bradshaw for their assistance in materials characterization.

**Conflicts of Interest:** The authors declare no conflict of interest.

#### References

1. Ezugwu, E.O. Key improvements in the machining of difficult-to-cut aerospace superalloys. *Int. J. Mach. Tools Manuf.* **2005**, *45*, 1353–1367. [[CrossRef](#)]
2. Heisel, U.; Lutz, M.; Spath, D.; Wassmer, R.A.; Walter, U. Application of minimum quantity cooling lubrication technology in cutting processes. *Prod. Eng.* **1994**, *2*, 49–54.
3. Filipovic, A.; Stephenson, D.A. Minimum quantity lubrication (MQL) applications in automotive power-train machining. *Mach. Sci. Technol.* **2006**, *10*, 3–22. [[CrossRef](#)]
4. Aronson, R.B. Why Dry Machining. *Manuf. Eng.* **1995**, *114*, 33–36.
5. Bennett, E.O.; Bennett, D.L. Occupational airway diseases in the metalworking industry Part 1: Respiratory infections, pneumonia, chronic bronchitis and emphysema. *Tribol. Int.* **1985**, *18*, 169–176. [[CrossRef](#)]
6. Brockhoff, T.; Walter, A. Fluid minimization in cutting and grinding. *Abrasives* **1998**, *10*, 38–42.
7. Jamadar, A.A.; Awale, V.S.; Kale, M.S. Minimum Quantity Lubrication. *Int. J. Adv. Res. Sci. Eng. Technol.* **2017**, *4*, 3150–3156.
8. Heinemann, R.; Hinduja, S.; Barrow, G.; Petuelli, G. Effect of MQL on the tool life of small twist drills in deep-hole drilling. *Int. J. Mach. Tools Manuf.* **2006**, *46*, 1–6. [[CrossRef](#)]
9. Attanasio, A.; Gelfi, M.; Giardini, C.; Remino, C. Minimal quantity lubrication in turning: Effect on tool wear. *Wear* **2006**, *260*, 333–338. [[CrossRef](#)]
10. Boubekri, N.; Shaikh, V. Machining using minimum quantity lubrication: A technology for sustainability. *Int. J. Appl. Sci. Technol.* **2012**, *2*, 111–115.
11. Yan, L.T.; Yuan, S.M.; Liu, Q. Effect of cutting parameters on minimum quantity lubrication machining of high strength steel. *Mater. Sci. Forum* **2009**, *626*, 387–392. [[CrossRef](#)]
12. Sharif, S.; Kurniawan, D.; Mohd, H.; Orady, E. Performance evaluation of vegetable oil as an alternative cutting lubricant when end milling stainless steel using TiAlN coated carbide tools. *Trans. N. Am. Manuf. Res. Inst. SME* **2009**, *37*, 9–14.
13. Mosleh, M.; Atnafu, N.D.; Belk, J.H.; Nobles, O.M. Modification of sheet metal forming fluids with dispersed nanoparticles for improved lubrication. *Wear* **2009**, *267*, 1220–1225. [[CrossRef](#)]
14. Sharma, A.K.; Tiwari, A.K.; Dixit, A.R. Improved machining performance with nanoparticle enriched cutting fluids under minimum quantity lubrication (MQL) technique: A review. *Mater. Today* **2015**, *2*, 3545–3551. [[CrossRef](#)]

15. Krishna, P.V.; Srikant, R.R.; Rao, D.N. Experimental investigation on the performance of nanoboric acid suspensions in SAE-40 and coconut oil during turning of AISI 1040 steel. *Int. J. Mach. Tools Manuf.* **2010**, *50*, 911–916. [[CrossRef](#)]
16. Vasu, V.; Kumar, K.M. Analysis of nanofluids as cutting fluid in grinding EN-31 steel. *Nano-Micro Lett.* **2011**, *3*, 209–214. [[CrossRef](#)]
17. Mosleh, M.; Ghaderi, M.; Shirvani, K.A.; Belk, J.; Grzina, D.J. Performance of cutting nanofluids in tribological testing and conventional drilling. *J. Manuf. Process.* **2017**, *25*, 70–76. [[CrossRef](#)]
18. Rahmati, B.; Sarhan, A.A.; Sayuti, M. Investigating the optimum molybdenum disulfide (MoS<sub>2</sub>) nanolubrication parameters in CNC milling of AL6061-T6 alloy. *Int. J. Adv. Manuf. Technol.* **2014**, *70*, 1143–1155. [[CrossRef](#)]
19. Moura, R.R.; da Silva, M.B.; Machado, Á.R.; Sales, W.F. The effect of application of cutting fluid with solid lubricant in suspension during cutting of Ti-6Al-4V alloy. *Wear* **2015**, *332*, 762–771. [[CrossRef](#)]
20. Xie, H.; Jiang, B.; Liu, B.; Wang, Q.; Xu, J.; Pan, F. An investigation on the tribological performances of the SiO<sub>2</sub>/MoS<sub>2</sub> hybrid nanofluids for magnesium alloy-steel contacts. *Nanoscale Res. Lett.* **2016**, *11*, 329. [[CrossRef](#)]
21. Hait, S.K.; Chen, Y. Study on the Influence of Li-Grease EP and AW Performance by Exfoliated MoS<sub>2</sub> Nanosheet Additive. *Adv. Sci. Lett.* **2014**, *20*, 1387–1395.
22. Mosleh, M.; Ghaderi, M. Deagglomeration of transfer film in metal contacts using nanolubricants. *Tribol. Trans.* **2012**, *55*, 52–58. [[CrossRef](#)]
23. Wojtewicz, M.; Nadolny, K.; Kapłonek, W.; Rokosz, K.; Matysek, D.; Ungureanu, M. Experimental studies using minimum quantity cooling (MQC) with molybdenum disulfide and graphite-based microfluids in grinding of Inconel<sup>®</sup> alloy 718. *Int. J. Adv. Manuf. Technol.* **2018**. [[CrossRef](#)]
24. Marques, A.; Suarez, M.; Sales, W.F.; Machado, A.R. Turning of Inconel 718 with whisker-reinforced ceramic tools applying vegetable-based cutting fluid mixed with solid lubricants by MQL. *J. Mater. Process. Technol.* **2019**, *266*, 530–543. [[CrossRef](#)]
25. Li, B.; Li, C.; Zhang, Y.; Wang, Y.; Jia, D.; Yang, M.; Zhang, N.; Wu, Q.; Han, Z.; Sun, K. Heat transfer performance of MQL grinding with different nanofluids for Ni-based alloys using vegetable oil. *J. Clean. Prod.* **2017**, *154*, 1–11. [[CrossRef](#)]
26. Paul, S.; Ghosh, A. Grinding of WC-Co cermets using hexagonal boron nitride nano-aerosol. *Int. J. Refract. Met. Hard Mater.* **2019**, *78*, 264–272. [[CrossRef](#)]
27. Le Coz, G.; Marinescu, M.; Devillez, A.; Dudzinski, D.; Velnom, L. Measuring temperature of rotating cutting tools: Application to MQL drilling and dry milling of aerospace alloys. *Appl. Therm. Eng.* **2012**, *36*, 434–441. [[CrossRef](#)]
28. Brinksmeier, E.; Janssen, R. Drilling of multi-layer composite materials consisting of carbon fiber reinforced plastics (CFRP), titanium and aluminum alloys. *CIRP Ann-Manuf. Technol.* **2002**, *51*, 87–90. [[CrossRef](#)]
29. Whinnem, E.; Lipczynski, G.; Eriksson, I. Development of orbital drilling for the Boeing 787. *SAE Int. J. Aerosp.* **2008**, *1*, 811–816. [[CrossRef](#)]
30. Ni, W. Orbital Drilling of Aerospace Materials. No. 2007-01-3814. *SAE Tech. Pap.* **2007**. [[CrossRef](#)]
31. Atarsia, A. Axial and Orbital Drilling of Thick Stacks for New Aircraft Assembly Process. *SAE Int. J. Aerosp. Eng.* **2013**, *6*, 540–544. [[CrossRef](#)]
32. Chang, C.H. Boelube R Dissolving Alkaline Cleaning Solution. U.S. Patent 6,240,935, 5 June 2001.
33. Gansheimer, J.; Holinsky, R. A study of solid lubricant in oils and greases under boundary conditions. *Wear* **1972**, *19*, 439–449. [[CrossRef](#)]
34. Hisakado, T.; Tsukizoe, T.; Yoshikawa, H. Lubrication mechanism of solid lubricants in oils. *J. Lubr. Technol.* **1983**, *105*, 245–253. [[CrossRef](#)]
35. Cizaire, L.; Vacher, B.; Le Mogne, T.; Martina, J.M.; Rapoport, L.; Margolinc, A.; Tennec, R. Mechanisms of ultra-low friction by hollow inorganic fullerene-like MoS<sub>2</sub> nanoparticles. *Surf. Coat. Technol.* **2002**, *160*, 282–287. [[CrossRef](#)]
36. Mosleh, M.; Belk, J.H. Methods and Compositions for Reducing Wear of Surfaces in Contact with One Another. U.S. Patent No. 9,605,228, 28 March 2017.
37. Gulzar, M.; Masjuki, H.H.; Varman, M.; Kalam, M.A.; Mufti, R.A.; Zulkifli, N.W.M.; Zahid, R. Improving the AW/EP ability of chemically modified palm oil by adding CuO and MoS<sub>2</sub> nanoparticles. *Tribol. Int.* **2015**, *88*, 271–279. [[CrossRef](#)]

38. Zhou, X.; Fu, X.; Shi, H.; Hu, Z. Lubricating properties of Cyanex 302-modified MoS<sub>2</sub> microspheres in base oil 500SN. *Lubr. Sci.* **2007**, *19*, 71–79.
39. Pawlak, Z.; Kaldonski, T.; Pai, R.; Bayraktar, E.; Oloyede, A. A comparative study on the tribological behaviour of hexagonal boron nitride (h-BN) as lubricating micro-particles—An additive in porous sliding bearings for a car clutch. *Wear* **2009**, *267*, 1198–1202. [[CrossRef](#)]



© 2019 by the authors. Licensee MDPI, Basel, Switzerland. This article is an open access article distributed under the terms and conditions of the Creative Commons Attribution (CC BY) license (<http://creativecommons.org/licenses/by/4.0/>).